SINTEZA ŞI PROPRIETĂȚILE FOTOCATALITICE ALE TiO_2 DOPAT CU Fe(III) PREPARAT PRIN METODA SOL-GEL

SYNTHESIS AND PHOTOCATALYTIC PROPERTIES OF Fe(III) - DOPED TiO_2 PREPARED BY SOL-GEL METHOD

OVIDIU OPREA[1], CRISTINA DANIELA GHIȚULICĂ[2*], GEORGETA VOICU[2], BOGDAN ŞTEFAN VASILE[2], ANGELICA OPREA[2]

[1]*Department of Inorganic Chemistry, Physical Chemistry and Electrochemistry, University Politehnica of Bucharest, Faculty of Applied Chemistry and Material Science, 1-7 Gh. Polizu Str., 011061 Bucharest, Romania*
[2] *Department of Science and Engineering of Oxide Materials and Nanomaterials, University Politehnica of Bucharest, Faculty of Applied Chemistry and Material Science, 1-7 Gh. Polizu Str., 011061 Bucharest, Romania*

Nanocatalysts of TiO_2 doped with 0.5% Fe (III) were prepared by the sol-gel method at 75°C. Titanium (IV) tetrabutoxide ($Ti(OC_4H_9)_4$), anhydrous iron (III) chloride ($FeCl_3$), acetic acid and acetyl acetone were used as starting materials. The synthesized materials were characterised by X-ray diffraction (XRD), transmission electron microscopy (TEM, HRTEM, SAED) and specific surface area by Brunauer, Emmett and Teller method (BET). The photocatalytic activity, measured by UV-Vis adsorption spectroscopy, was evaluated by the photocatalytic degradation of methylene blue (MB) in water under UV irradiation. From XRD and SAED analyses, the results indicate that anatase was obtained at temperature up to 800°C; above this temperature the rutile was obtained, with low photocatalytic properties. The TEM, HRTM and BET analyses showed the presence of nano size and mesoporous particles with high surface area.

Nanocatalizatorii de TiO_2 dopat cu 0,5% Fe (III) au fost preparați prin metoda sol-gel la 75°C. Ca materii prime s-au utilizat: tetrabutoxidul de titan ($Ti(OC_4H_9)_4$), clorura ferică anhidră ($FeCl_3$), acidul acetic şi acetil acetona. Materialele sintetizate au fost caracterizate prin difracție de raze X (XRD), microscopie electronică de transmisie (TEM, HRTEM, SAED) şi suprafață specifică utilizând meoda Brunauer-Emmett-Teller (BET). Activitatea fotocatalitică măsurată prin adsorbție UV-Vis, a fost evaluată prin degradarea fotocatalitică a albastrului de metil (MB) în apă sub iradiere UV. Din analizele XRD şi SAED, rezultă că până la temperatura de 800°C se obține faza anatas, iar peste această temperatură se formează şi rutilul, care are proprietăți fotocatalitice mai slabe. Analizele TEM, HRTM şi BET arată prezența de nanoparticule mezoporoase cu suprafață specifică mare.

Keywords: *sol-gel method, anatase, rutile, Fe-doping, photocatalytic properties*

1. Introduction

Titanium dioxide is one of the semiconductor oxides with biological properties and with different applications (e.g. liquid solar cell [1], gas sensors [2, 3], degradation of toxic materials and pollutants [4-7], as well as a very good support for osteoblastic cell attachment [8-10]. It has three polymorphic forms: anatase (tetragonal), rutile (tetragonal) and brookite (orthorhombic). For the above mentioned applications, only anatase and rutile are used, because brookite phase is stable only at very low temperatures and hence not so useful practically.

The anatase phase presents photocatalytic properties due to large band gape energy (3.2 eV) and it is active only under ultraviolet light (UV) irradiation, corresponding to 388 nm. The ultimate purpose is the direct utilization of solar energy, but the solar spectrum is relatively poor in UV light (approx. 4%) at the surface on Earth. An other difficulty with TiO_2 is the high recombination rate of the photoexcited electron–hole pairs in the irradiated particles. The fast recombination is in competition with the reactions of decomposing the pollutants. To solve these problems researchers tried changing the electronic structure of the photocatalyst by doping TiO_2 with transition metal ions. Recent studies show that iron (III) ion seems to be the most suitable for this purpose[4-11].

Therefore, the aim of this work was to obtain nanocatalysts of TiO_2 doped with 0.5% Fe (III) by the modified sol-gel method using delaying agents of hydrolysis and polycondensation processes. The structure of nanocatalysts was characterised by X-ray diffraction (XRD), transmission electron microscopy (TEM, HRTEM, SAED) and nitrogen adsorbtion-desorbtion isotherms (BET). To deter-

* Autor corespondent/Corresponding author,
Tel. . +40 214023984, e-mail: cghitulica@yahoo.com

mine the relationship between thermal treatment conditions and photocatalytic properties of these materials were performed spectrophotometric analyses after degradation of methylene blue under UV irradiation.

2. Experimental

2.1. Preparation of materials

The TiO_2 doped with 0.5% Fe (III) were obtained by the sol-gel method presented in Figure 1. The reagents were: titanium tetrabutoxide ($Ti(OBu)_4$, Sigma Aldrich; 97%) and anhydrous iron (III) chloride ($FeCl_3$, Chemical Company; 98%). As delaying agents of hydrolysis and polycondensation processes were used acetic acid ($C_2H_4O_2$, Sigma Aldrich; 99.8%; used to ensure acidic conditions, too) and acetylacetone ($C_5H_8O_2$, Sigma Aldrich, ≥99.5%; used as sol stabilization agent). As solvents were used 2-propanol (C_3H_8O, Sigma Aldrich) and distilled water.

$Ti(OBu)_4$ was mixed with 2-propanol and in this solution was dissolved $FeCl_3$ under vigorous magnetic stirring, at 75°C under refluxing. Also, $C_2H_4O_2$ and $C_5H_8O_2$ were added (under magnetic stirring) until a light reddish solution was obtained; this solution was homogenised 24 h under the same conditions. After 24h, water was added and solution was continuously stirred at 75°C, for 1 hour, under refluxing. The remaining alcohol was evaporated in order to accelerate the polycondensation reaction, and a viscous reddish gel was formed. This gel was then dried at 100°C for 72 hours resulting a dark reddish powder resin.

This dark reddish resin was investigated by the thermal treatment (DTA/TG) and X-ray diffraction analysis (XRD). The resin was thermally treated at 500°C/2h (v=5°C/min) for the dissociation of polymer network and burning of the organic material. The resulting powder was investigated by XRD and transmission electron-microscopy and then calcined in different conditions: 500°C for 2h and 4h; 800°C for 2h and 4h. The calcined specimens were subjected to a slow cooling in furnace. The resulted powders were investigated by XRD and nitrogen adsorption–desorption isotherms (BET).

2.2. Characterization

The thermal analysis (DTA/TG) was performed using a Shimadzu DTG-TA-60, in the 20-1000°C temperature range, with a heating rate of 10°C/min, in air.

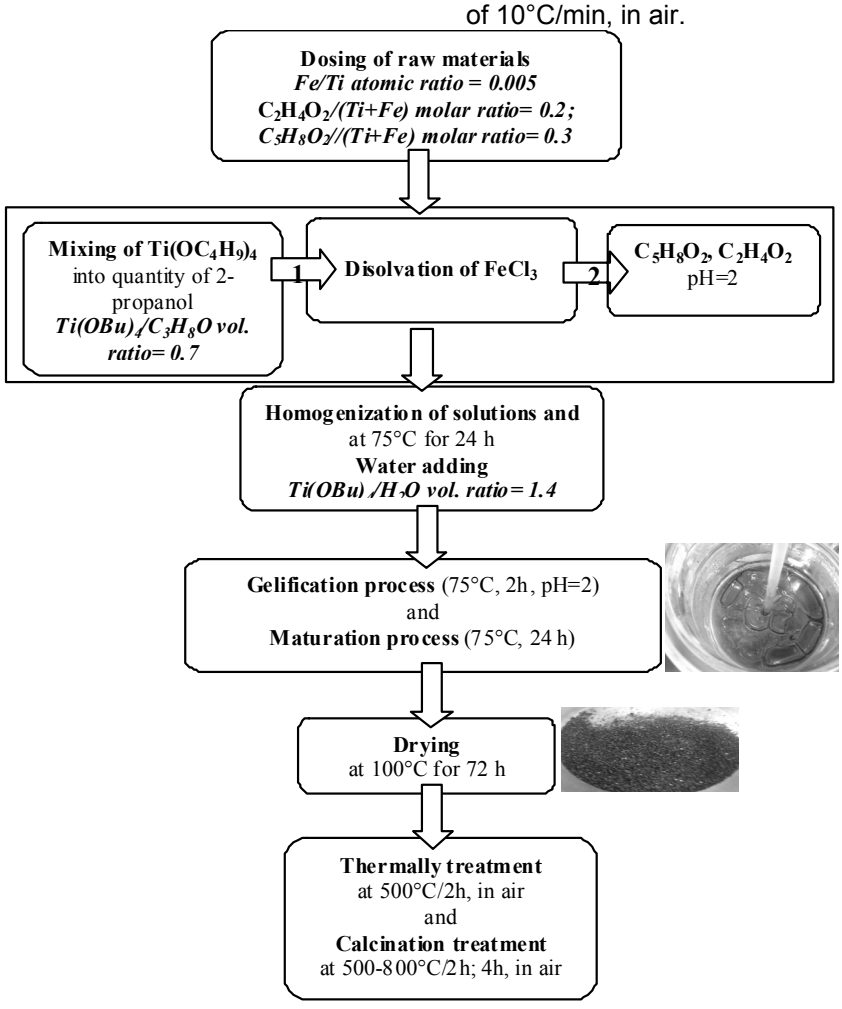

Fig. 1 - The obtaining of TiO_2 doped with 0.5% Fe (III) nanocatalysts by sol-gel method./ *Schema de obţinerea de nanocatalizatori de TiO_2 dopat cu 0,5% Fe (III) prin metoda sol-gel.*

For the identification of crystalline phases of powders, X-ray diffraction analysis was carried out on a Shimadzu diffractometer XRD 6000 - Ni-filtered CuKα (λ = 1.5406 Å) radiation, scanning speed of 2 deg./min in 2θ range of 10 - 80 deg.

In order to estimate both the average particle size and the crystallinity degree TEM-SAED/HRTEM investigations were performed, using a TecnaiTM G^2 F30 S-TWIN high resolution transmission electron microscope (HR-TEM) equipped with STEM—HAADF detector, EDX and EELS.

Specific surface areas of photocatalysts were determined using a Micromeritics- Gemini Type 2380 gas adsorption analyzer at 77K in liquid nitrogen. The powders were pretreated in a vacuum at 80°C for 24 h. The pore-size distributions and the specific areas were estimated using Brunauer-Emmet-Teller method (BET).

For determination of photocatalytic activity, samples of 0.0250 g powder were immersed in 20 mL solution of methylene blue 0.001%. The photocatalytic activity was evaluated spectrophotometrically after degradation of methylene blue (MB) under UV irradiation; the spectra were recorded with a JASCO V560 spectrophotometer, in the domain 200-800 nm, with a speed of 200 $nm \cdot min^{-1}$.

3. Results and discussion

The X-ray diffraction of dark reddish resin is displayed in Figure 2. It can be seen that the peaks specific for titanium oxide with anatase structure (JCPDS 21-1272) are present in the XRD spectra and average crystallite size estimated by Debye-Scherrer equation is 4.23 nm.

The TEM image, presented in Figure 3a, shows almost unisolated particles, with non-uniform shapes. However, some better-defined particles (black circles) allowed to roughly estimate an equivalent size of 4.23 nm, close to the average crystallite size value calculated from the XRD data, suggesting that prior to form aggregates, the individual particles seem to be single crystals. The HRTEM image (Figure 3b) shows the presence of individual, small crystallites and the ordered fringes spaced at 3.52 Å, corresponding to the (101) crystalline planes of the anatase structure. The SAED pattern presented in Figure 3c, indicate the lightly-marked diffraction rings (probably due to the small size of the crystallites) and a polycrystalline character of the dark reddish resin.

The thermal analysis of dark reddish resin presented in Figure 4 indicates a total weight loss of 24.92%. The DTA-TG curves reveal an important exothermic effect at 231.3°C accompanied by weight loss (19.34%) in the temperature range of 150 – 500°C that is attributed to the decomposition of the organic part of the precursor. The small endothermic effects at 573.2°C and 826.1°C accompanied by low weight loss (2.71%) in the range 500-1000°C are attributed to residual, amorphous carbonaceous mass decomposition, present under the detection limit of the diffractometer.

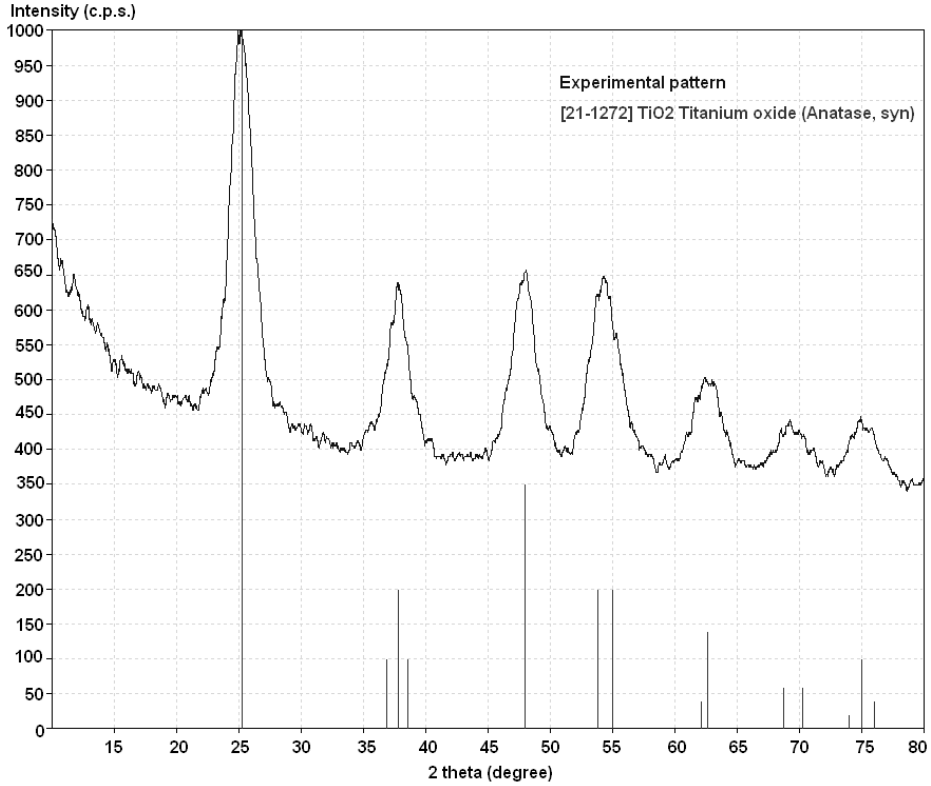

Fig. 2 - The XRD pattern of dark reddish resin/ *Imaginea de difracție de raze X caracteristică răşinii de culoare roşcat închis.*

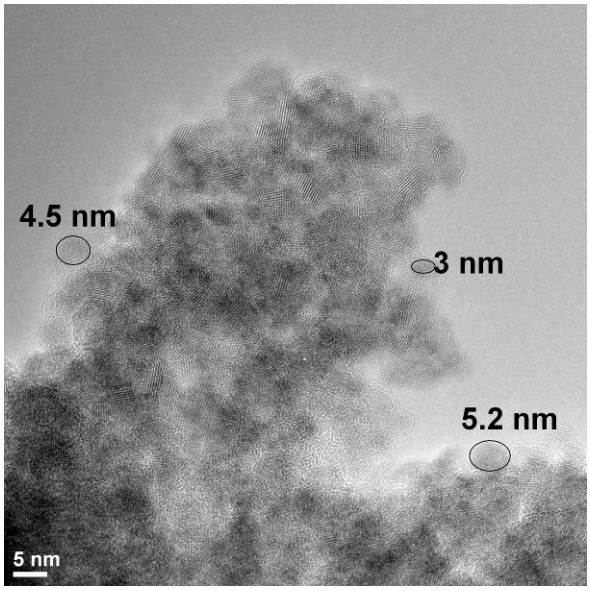

a

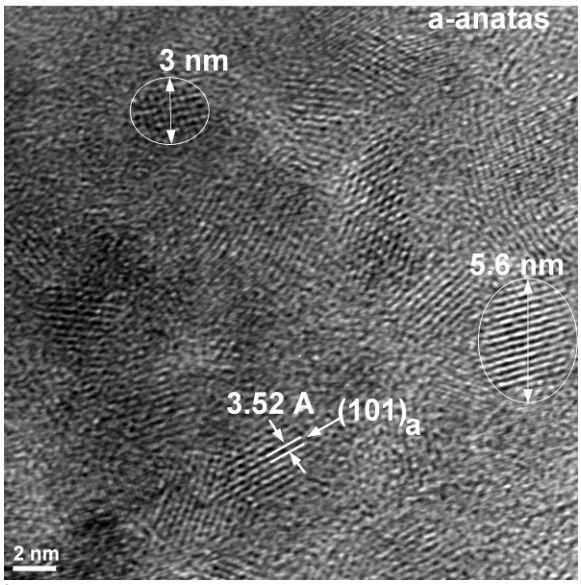

b

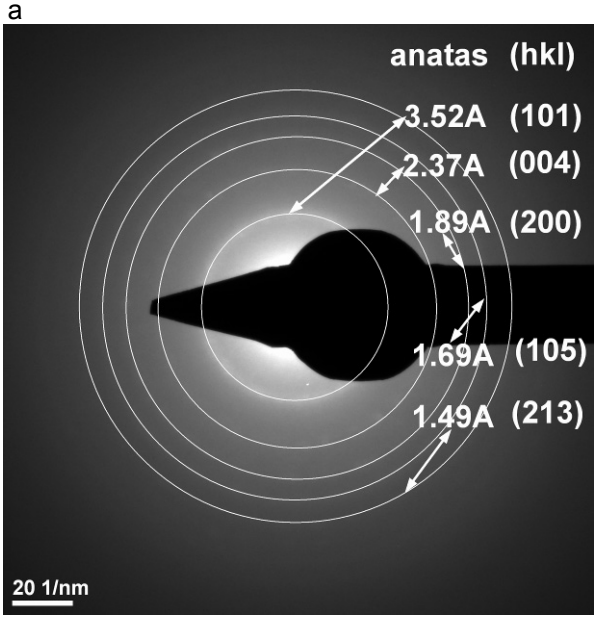

c

Fig. 3 - Transmission electron microscopy images for dark reddish resin: (a) TEM image; (b) HR-TEM image; (c) SAED pattern./ *Imaginile de microscopie electronică de transmisie pentru răşina de culoare roşcat închis: (a) imagine TEM; (b) imagine HR-TEM; (c) analiză SAED.*

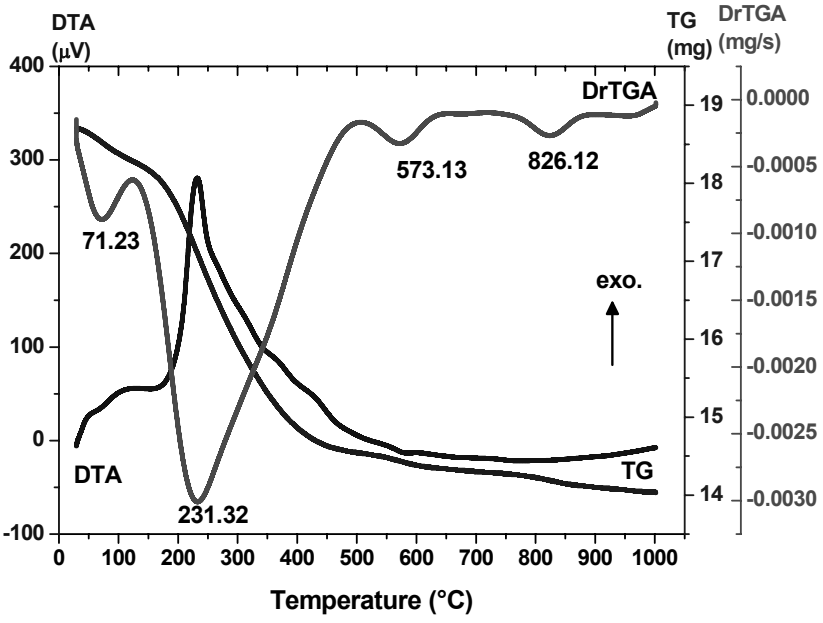

Fig. 4 - Thermal analysis of dark reddish resin./*Analiză termică a răşinii de culoare roşcat închis.*

The thermal analysis of dark reddish resin presented in Figure 4 indicates a total weight loss of 24.92%. The DTA-TG curves reveal an important exothermic effect at 231.3°C accompanied by weight loss (19.34%) in the temperature range of 150 – 500°C that is attributed to the decomposition of the organic part of the precursor. The small endothermic effects at 573.2°C and 826.1°C accompanied by low weight loss (2.71%) in the range 500-1000°C are attributed to residual, amorphous carbonaceous mass decomposition, present under the detection limit of the diffractometer.

Therefore, the dark reddish resin was thermal treated at 500°C for 2 h in order to achieve the decomposition of the organic part. The powder obtained has a light grey colour suggesting the presence of very low amount of carbon. This powder was analised by XRD- Figure 5, and transmission electron-microscopy - Figure 6. On the X-ray diffraction spectra are present only the peaks specific for titanium oxide with anatase structure (JCPDS 21-1272) and the average crystallite size estimated by Debye-Scherrer equation is 12.05nm. As expected, with increase of thermal temperature treatment the crystalline

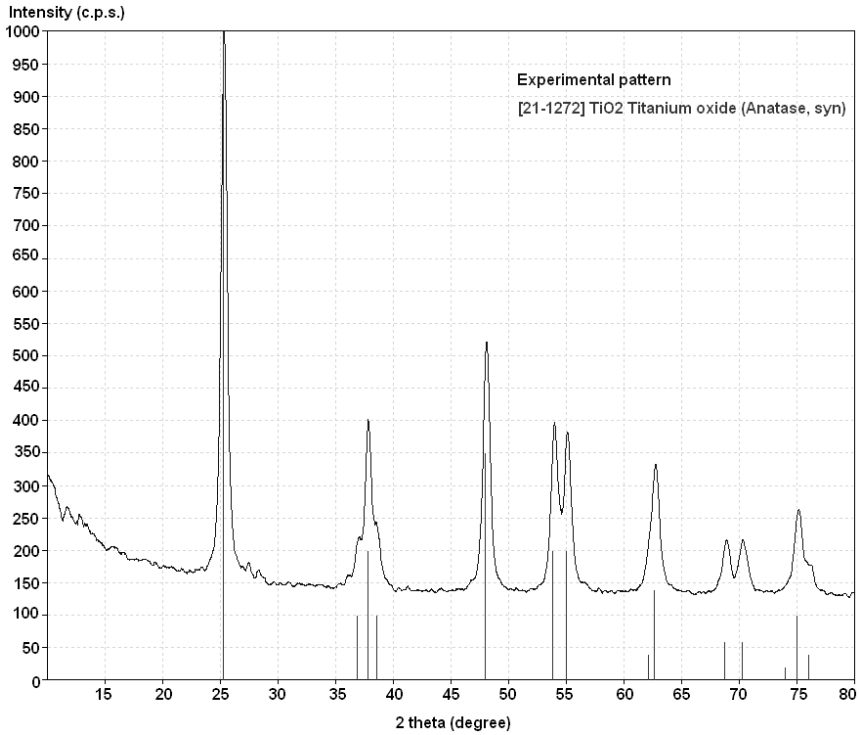

Fig. 5 - The XRD pattern of light grey powder./ *Imaginea de difracție de raze X caracteristică pulberii de culoare gri deschis.*

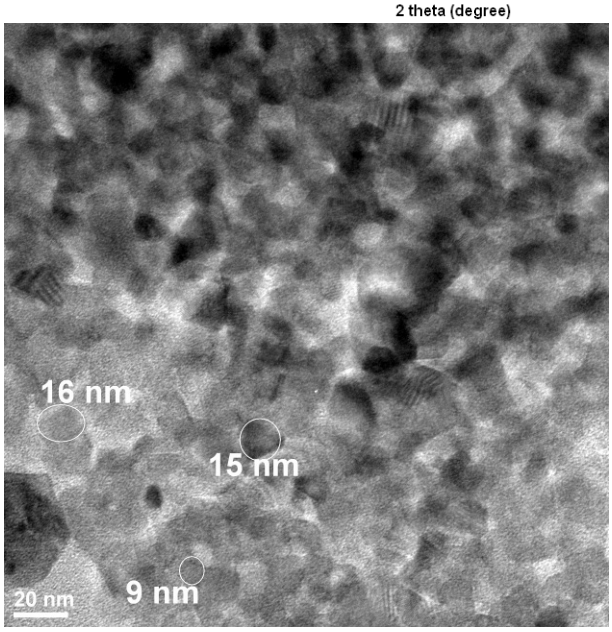

a

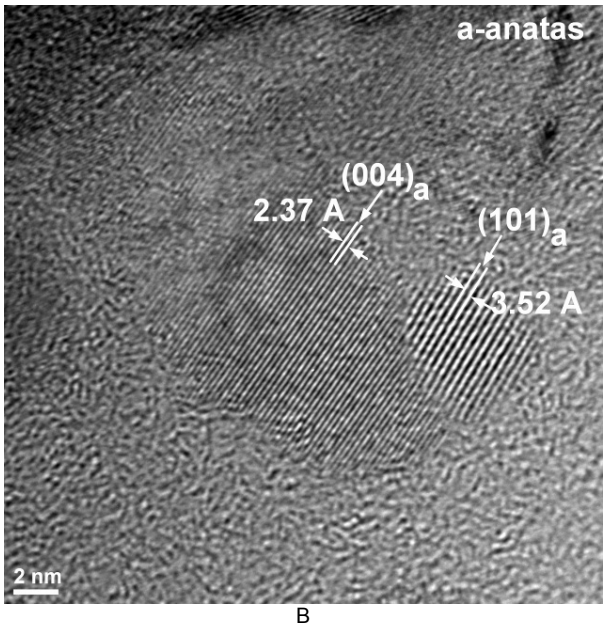

B

Figura 6 (continuare pe pagina următoare / *continues on the next page*)

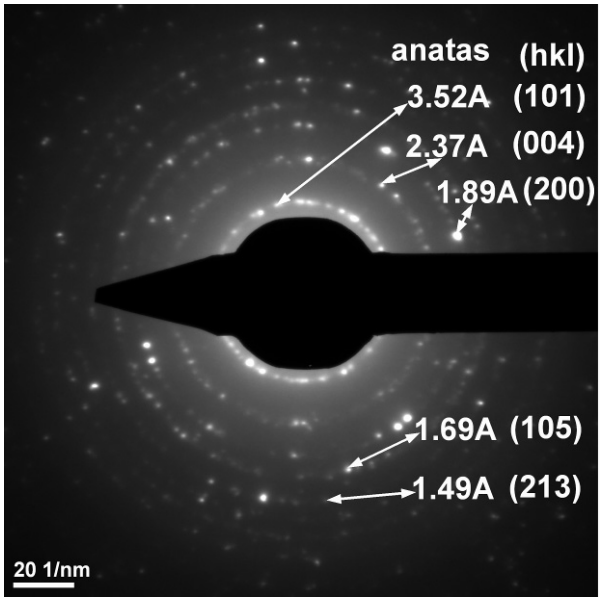

c

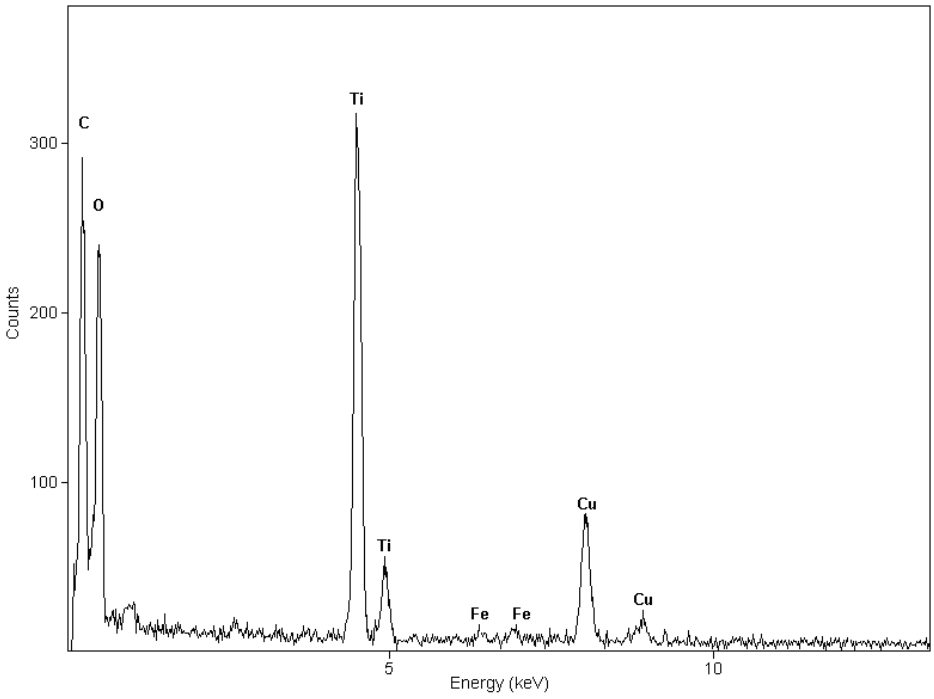

d

Fig. 6 - Transmission electron microscopy images for light grey powder: (a) TEM image; (b) HR-TEM image; (c) SAED pattern; (d) EDX spectrum./ *Imaginile de microscopie electronică de transmisie pentru pulberea de culoare gri deschis: (a) imagine TEM; (b) imagine HR-TEM; (c) analiză SAED; (d) spectru EDX.*

degree increases. This is in agreement with transmission electron-microscopy images, were it can be observed an increase of grain average size up to 13.33 nm- Figure 6a and the polycrystalline nature of nanocatalyst- Figure 6b, c. In addition, the energy-dispersive X-ray spectroscopy (EDX) – Figure 6d, shows a Ti/Fe atomic ratio in good agreement with initial data (see Figure 1).

The light grey powder was calcined at 500°C for 2h and 4h, and 800°C for 2h and 4h and the X-ray patterns of these samples are presented in Figure 7. The increase of the plateau from 2h to 4h leads to the increase of the crystallinity degree. In addition, increase of thermal temperature treatment from 500°C to 800°C induces polymorph transformation of anatase (JCPDS 21-1272) to rutile (JCPDS 78-2485). Transmission electron-microscopy images for grey powder thermally treated at 500°C for 4h indicate an increase in the average grain size up to approx. 18.5 nm- Figure 8a, and polycrystalline nature of the nanocatalyst- Figure 8b, c that is in agreement with X-ray analysis. The energy-dispersive X-ray spectroscopy (EDX) – Figure 8d, shows a Ti/Fe atomic ratio which is the same as the one designed.

In the Table 1 are shown the BET data - specific surface area, average pore diameter and the primary particle size (D_{BET}) of the powders thermal treated at 500°C. D_{BET} was calculated by assuming the primary particles to be spherical with relation [12, 13]: $D_{BET}=6\cdot10^3/(S\cdot\rho)$ (nm), where: ρ-is the theoretical density of compounds (g/cm^3) and S is the BET specific surface area (m^2/g). One can

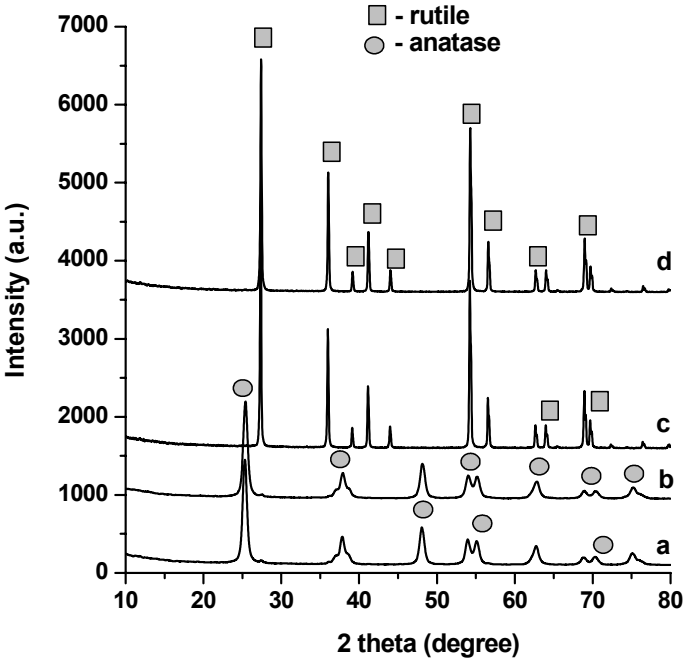

Fig. 7 - The XRD patterns of the light grey powder thermal treated at: 500°C for 2h (a) and 4h (b); 800°C for 2h (c) and 4h (d)./ *Imaginile de difracție de raze X caracteristice pulberii de culoare gri deschis tratată termic la: 500°C pentru 2h (a) şi 4h (b); 800°C pentru 2h (c) şi 4h (d).*

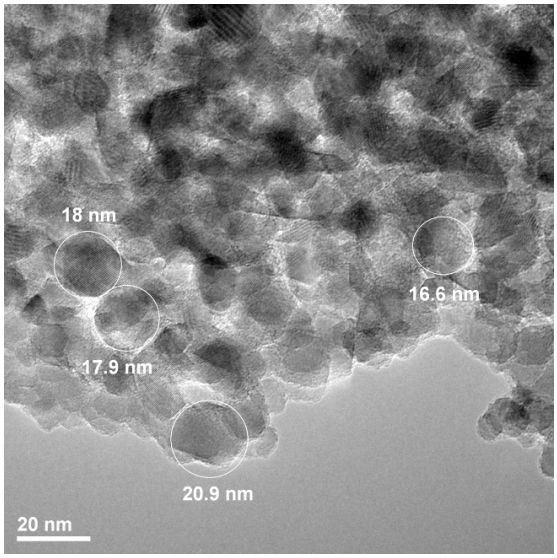

a

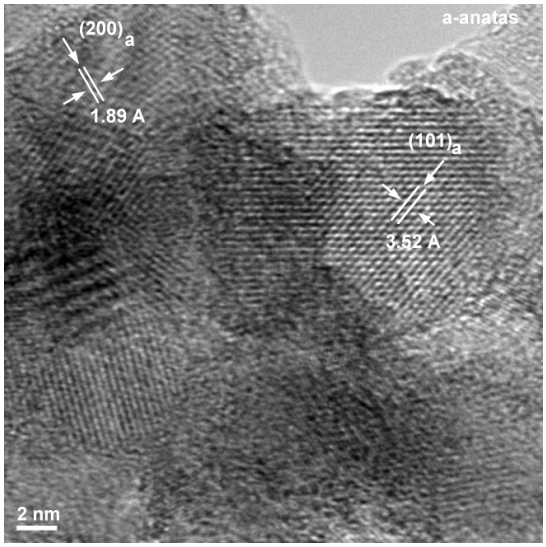

b

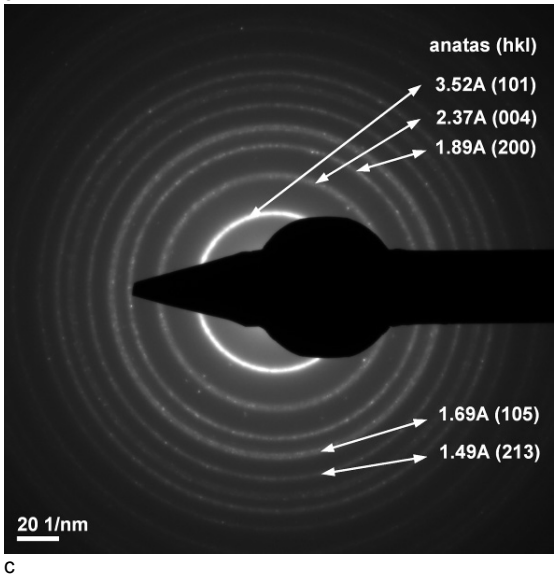

c

Fig. 8 - Transmission electron microscopy images for the light gray powder thermal treated at 500°C for 4 h: (a) TEM image; (b) HR-TEM image; (c) SAED pattern; (d) EDX spectrum./ *Imaginile de microscopie electronică de transmisie pentru pulberea de culoare gri deschis tratată termic la 500°C pentru 4 h: (a) imagine TEM; (b) imagine HR-TEM; (c) analiză SAED; (d) spectru EDX.*

Fig.8 se continuă pe pagina următoare
Fig. 8 continues on the next page.

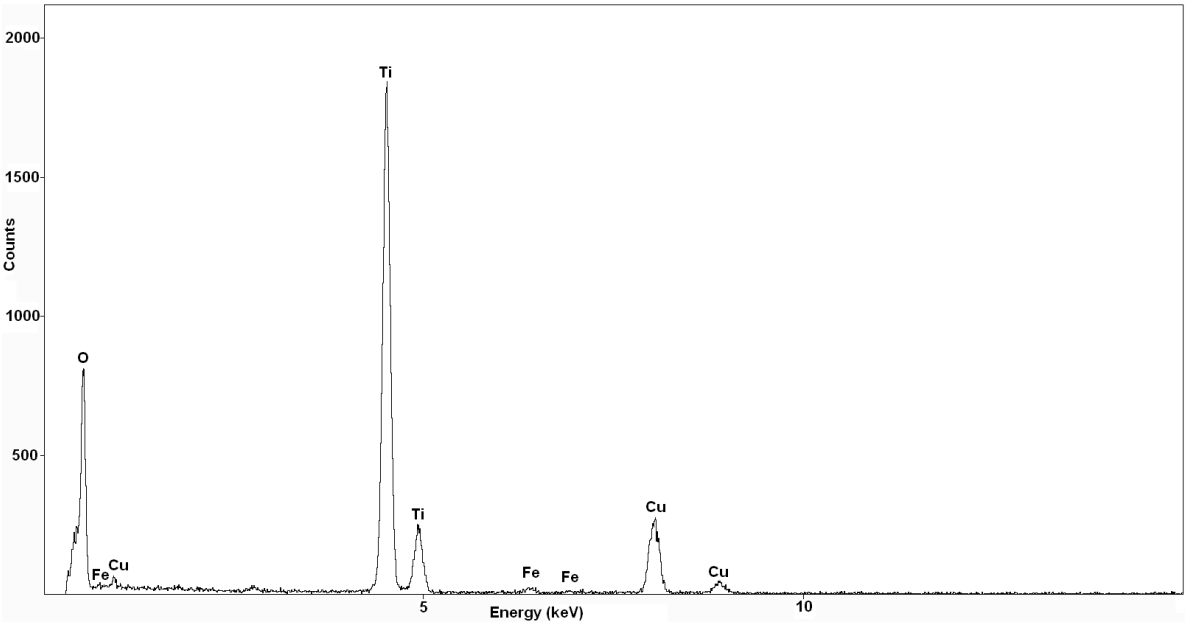

Fig. 8d

Table 1

The BET data of the powders thermal treated at 500°C.
Date BET ale pulberii tratate termic la 500°C.

Samples *Probele*	BET surface area *Aria specifică BET* (m^2/g)	BJH Adsorption average pore diameter (4V/A) / *Diametrul mediu al porilor prin adsorbţie BJH* (nm)	Primary particle size, *Dimensiunea de paticulă* D_{BET} (nm)
Gray powder *Pulbere gri*	91.71	6.77	16.8
500°C/2h	68.73	8.02	22.4
500°C/4h	68.52	7.98	22.5

observe high values of specific surface area and small values of average pore diameter; these characteristics are assumed to have a good influence on the photocatalytic activity.

The photocatalytic activity versus irradiation time is presented in Figure 9 considering the absorption band from 658 nm [14]. All samples have good photocatalytic activity, the highest activity being measured for light grey powder calcined at 500°C for 4h. For the same thermal treatment temperature (500°C), the increase of the plateau induces the increase of photocatalytic activity; this is due to the decrease of the carbon content, which blocks the nanoparticles surface.

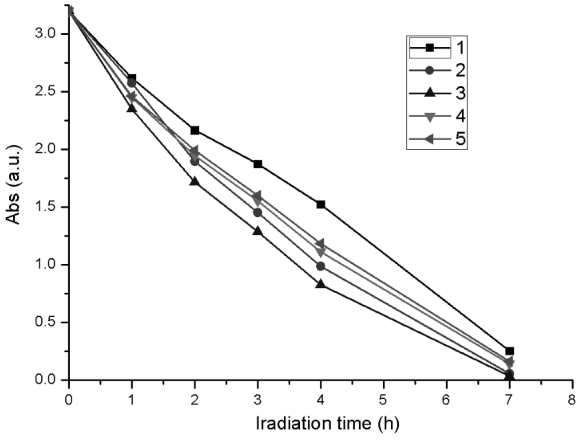

Fig. 9 - The photocatalytic activity versus irradiation time for dark reddish resin thermal treated at 500°C for 2h (1) and light gray powder thermal treated at: 500°C for 2h (2) and 4h (3); 800°C for 2h (4) and 4h (5) (absorption band at 658 nm)./*Activitatea fotocatalitică funcţie de timpul de iradiere pentru răşina de culoare roşcat închis tratată termic la 500°C pentru 2h (1) şi pulberea gri deschis tratată termic la 500°C pentru 2h (2) şi 4h (3); 800°C pentru 2h (4) şi 4h (5) (banda de absorţie de la 658 nm).*

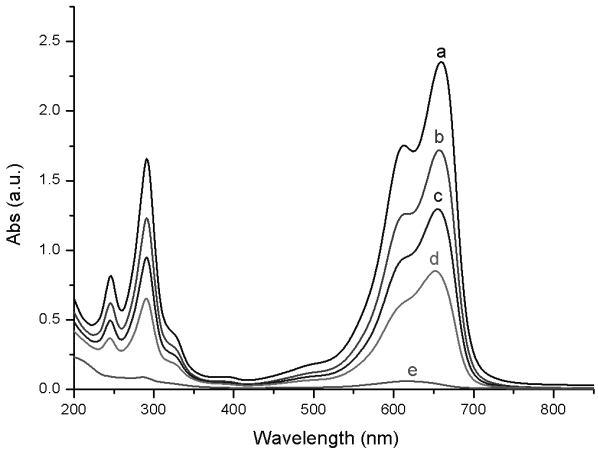

Fig. 10 - The photocatalytic activity versus irradiation time (a- 1 h; b – 2 h; c – 3 h; d – 4 h; e – 7 h) for light gray powder thermal treated at 500°C for 4h./ *Activitatea fotocatalitică funcţie de timpul de iradiere (a- 1 h; b – 2 h; c – 3 h; d – 4 h; e – 7 h) pentru pulberea de culoare gri deschis tratată termic la 500°C pentru 4 h.*

Increase of thermal treatment temperature from 500°C to 800°C, induced changes of the parameters lattice from anatase to rutile, which according to the literature data [1, 15-21] decrease of photocatalytic activity. In Figure 10 is presented the photocatalytic activity versus irradiation time (from 1 to 7 hours) for light grey powder thermal treated at 500°C/4h. The absorbance values diminish from 1h up to 7h reaction, what indicated that MB in water has been entirely degraded.

4. Conclusions

Nanocatalysts of TiO_2 doped with 0.5% Fe (III) were prepared by the sol-gel method at 75°C. The anatase phase was obtained by thermal treatment at 500°C and has high specific surface area (91.71 m^2/g for the sample treated at 500°C for 2h). For the same thermal treatment temperature (500°C), the increase of the thermal treatment plateau to 4h induces the increase of photocatalytic activity of nanocatalysts; this is due to the decrease of the carbon content, which blocks the nanoparticles surface. The rutile phase is formed when the treatment is performed at 800°C and as expected has low photocatalytic properties.

Acknowledgements

This paper is supported by the Sectoral Operational Programme Human Resources Development, financed from the European Social Fund and by the Romanian Government under the contract number POSDRU/86/1.2/S/58146 (MASTERMAT).

REFERENCES

1. S. Ito, P. Chen, P. Comte, M. K. Nazeeruddin, P. Liska, P. Péchy, and M. Grätzel, Fabrication of screen-printing pastes from TiO_2 powders for dye-sensitised solar cells, Progress in Photovoltaics: Research and Applications, 2007, **15**, 603.
2. R. Ramamoorthy, P.K. Dutta, and S.A. Akbar, Oxygen sensors: Materials, methods, designs and applications, Journal of Materials Science, 2003, **38**, 4271.
3. S. Lin, D. Li, J. Wu, X. Li, S.A. Akbar, A selective room temperature formaldehyde gas sensor using TiO_2 nanotube arrays, Sensors and Actuators B: Chemical, 2011, 156, 505.
4. X. Lu, Y. Ma, B. Tian, and J. Zhang, Preparation and characterization of Fe-TiO_2 films with high visible photoactivity by autoclaved-sol method at low temperature, Solid State Sciences, 2011, **13**, 625.
5. C-H. Lu, C.-Y. Hu, and C-H. Wu, Low-temperature preparation and characterization of iron-ion doped titania thin films, Journal of Hazardous Materials, 2008, 159, 636.
6. E. B. Azevedo, F.R. de Aquino Neto, and M. Dezotti, TiO_2-photocatalyzed degradation of phenol in saline media: lumped kinetics, intermediates, and acute toxicity, Applied Catalysis B: Environmental, 2004, **54**, 165.
7. S. Irmak, E. Kusvuran, and O. Erbatur, Degradation of 4-chloro-2-methylphenol in aqueous solution by UV irradiation in the presence of titanium dioxide, Applied Catalysis B: Environmental, 2004, **54**, 85.
8. T. Miyauchi, M. Yamada, A. Yamamoto, F. Iwasa, T. Suzawa, R. Kamijo, K. Baba, and T. Ogawa, The enhanced characteristics of osteoblast adhesion to photofunctionalized nanoscale TiO_2 layers on biomaterials surfaces, Biomaterials, 2010, **31**, 3827.
9. H-J. Oh, J-H. Lee, Y-J. Kim, S-J. Suh, J-H. Lee, and C-S. Chi, Surface characteristics of porous anodic TiO_2 layer for biomedical applications, Materials Chemistry and Physics, 2008, 109, 10.
10. J-X. Wang, Y-B. Fan, Y. Gao, Q-H. Hu, and T-C. Wang, TiO_2 nanoparticles translocation and potential toxicological effect in rats after intraarticular injection, Biomaterials, 2009, **30**, 4590.
11. Z. Ambrus, N. Balázs, T. Alapi, G. Wittmann, P. Sipos, A. Dombi, and K. Mogyorósi, Synthesis, structure and photocatalytic properties of Fe(III)-doped TiO_2 prepared from $TiCl_3$, Applied Catalysis B: Environmental, 2008, **81**, 27.
12. F.B. Ayed, J. Bouaziz, and K. Bouzouita, Calcination and sintering of fluorapatite under argon atmosphere, J. Alloys Compd., 2001, **322**, 238.
13. F.B. Ayed, and J. Bouaziz, Sintering of tricalcium phosphate–fluorapatite composites with zirconia, Journal of the European Ceramic Society, 2008, **28**, 1995.
14. G. Voicu, O.Oprea, B.S. Vasile, and E. Andronescu, Photoluminescence and photocatalytic activity of Mn-doped ZnO nanoparticles", Digest Journal of Nanomaterials and Biostructures, 2013, **8** , 667.
15. M. Răileanu, M. Crişan, I. Niţoi, A. Ianculescu, P. Oancea, D. Crişan, and L. Todan, TiO_2-based nanomaterials with photocatalytic properties for the advanced degradation of xenobiotic compounds from water. a literature survey, Water, Air and Soil Pollution, 2013, **224**, 1548.
16. W.J. Tseng, and P-S. Chao, Synthesis and photocatalysis of TiO_2 hollow spheres by a facile template-implantation route, Ceramics International, 2013, **39**, 3779.
17. X. Chen, and S.S. Mao, Titanium dioxide nanomaterials: synthesis, properties, modifications and applications, Chemical Reviews, 2007, **107**, 2891.
18. M. Răileanu, M. Crişan, N. Drăgan, D. Crişan, A. Galtayries, A. Brăileanu, A. Ianculescu, V.S. Teodorescu, I. Niţoi, and M. Anastasescu, Sol–gel doped TiO_2 nanomaterials: a comparative study, Journal of Sol-Gel Science and Technology, 2009, **51**, 315.
19. J.H. Jho, D.H. Kim, S-J. Kim, and K.S. Lee, Synthesis and photocatalytic property of a mixture of anatase and rutile TiO_2 doped with Fe by mechanical alloying process, Journal of Alloys and Compounds, 2008, **459**, 386.
20. S. Tieng, A. Kanaev, and K. Chhor, New homogeneously doped Fe(III)–TiO_2 photocatalyst for gaseous pollutant degradation, Applied Catalysis A: General, 2011, **399**, 191.
21. É.G. Bajnóczi, N. Balázs, K. Mogyorósi, D.F. Srankó, Z. Pap, Z. Ambrus, S.E. Canton, K. Norén, E. Kuzmann, A. Vértes, Z. Homonnay, A. Oszkó, I. Pálinkó, and P. Sipos, The influence of the local structure of Fe(III) on the photocatalytic activity of doped TiO_2 photocatalysts—An EXAFS, XPS and Mössbauer spectroscopic study, Applied Catalysis B: Environmental, 2011, **103**, 232.

****